I hereby certify that this correspondence is being deposited with the United States Postal Service on the date set forth below as First Class Mail in an envelope addressed to: Commissioner for Patents, P.O. Box 1450, Alexandria, VA 22313-1450.

Date of Signature and Deposit: 7/20/06

Jack M. Cook, Reg. No. 56,098

IN THE UNITED STATES PATENT AND TRADEMARK OFFICE

Applicant:	Boris A. Shoykhet
Serial No.:	10/761,716
Filed:	January 21, 2004
Title:	Joint Assembly for Superconducting Motors
Art Unit:	2834
Examiner:	Thanh Lam
Attorney Docket:	110003.95637 (97RE027-B)

DECLARATION UNDER 37 C.F.R. 1.132

Commissioner for Patents
P.O. Box 1450
Alexandria VA 22313-1450

Dear Sir:

I, Boris A. Shoykhet, declare and say that:

1. I am the named inventor of the invention claimed in the above-listed patent application.

2. Meyer et al. (U.S. Patent No. 5,283,941) is directed to a method for brazing end rings and rotor bars formed of similar materials for use in a traditional (i.e., non-superconducting) motor.

3. Meyer et al. teaches the use of similar (i.e., not dissimilar) materials to form rotor bars and end rings. In particular, Meyer et al. teaches that the rotor bars and end rings should both be formed of chrome copper alloy or both be formed of copper or copper alloys. *See* col. 1, ll. 19-40. On the other hand, the claims of the present invention are clear that dissimilar materials are utilized to create a joint that is substantially free of singularities.

4. Meyer et al. does not deal with the difficulties presented when joining or bonding dissimilar materials, such as my invention seeks to overcome. Rather, Meyer et al. produces joints without unduly weakened bonds by controlling "overaging or overaged temperatures." *See* col. 1, ll. 34-40 and col. 2, ll. 23-27. One of ordinary skill in the art would readily recognize that the control of "overaging or

overaged temperatures" taught by Meyer et al. would not yield the claimed joint formed by dissimilar materials that is substantially free of singularities.

5. One of skill in the art would readily recognize that superconducting motors are subject to a wide variety of operational and environmental constraints that are not present in other motor systems.

6. Meyer et al. does not teach or suggest the applicability of any brazing methods to the specific constraints of superconducting motors. On the other hand, the pending claims explicitly call for the applicability of the invention to superconducting motors and/or the use of the invention under the operational constraints and within environments of superconducting motors.

7. I have reviewed the prior art of record and believe that it does not disclose or suggest my invention as claimed. Accordingly, I request that a patent be granted for my invention.

8. I hereby declare that all statements made herein of my own knowledge are true and that all statements made on information and belief are believed to me to be true; and further that these statements are made with the knowledge that willful false statements and the like so made are punishable by fine or imprisonment, or both, under Section 1001 of Title 18 of the United States Code and that such willful false statements may jeopardize the validity of the application or any patent issuing thereon.

Dated: 07/17/2006

Boris A. Shoykhet

Boris A. Shoykhet

Design and Testing of a 1,000-HP High-Temperature Superconducting Motor

Viatcheslav Dombrovski*, *Member, IEEE*, David Driscoll*, Boris Shoykhet*,
Stephen Umans, *Fellow, IEEE* and Joe Zevchek*

***Abstract*—A synchronous motor with a high-temperature superconducting field winding has been successfully constructed and tested. Designed to produce an output power of 1,000 hp, this motor was operated successfully at this power rating and achieved an output power of 1,600 hp during subsequent testing. This paper provides an overview of the design of the motor and discusses the results of a series of tests which were performed on the motor.**

***Index Terms*—Synchronous motors, High-temperature superconductors, AC motors**

I. Introduction

THE development effort for super-efficient electric motors started in 1987, shortly after the discovery of high-temperature superconducting (HTS) materials in 1986. The higher operating temperature of HTS materials, as compared to previous superconductors that required liquid-helium cooling at 4.2 K, results in lower cooling costs to maintain the coils in their superconducting state. For superconducting rotating machinery, the lower cooling costs provide the potential to reduce the rating of economically-viable products from the hundreds of megawatt range of central station generators to the thousands of horsepower range of large electric motors.

It has been estimated that superconducting motors offer benefits in the form of a reduction of 50% in both losses and size compared to conventional motors of the same rating [1]. Thus, the expected benefits of HTS motors are higher motor efficiency and smaller motor size. Both of these benefits are a direct result of being able to use the HTS motor field winding to create a high magnetic field [2]. Possible markets for superconducting motors include pumps, fans, and compressors for utility and industrial applications where continuous operation and minimal maintenance are expected.

The goal of the 1,000-hp HTS motor development was to demonstrate an HTS motor comparable with conventional motors in terms of efficiency and size for the same power rating. The development of this motor involved a collaboration of six team members from industry, utility companies and government laboratories. Features of significance associated with this motor include a closed-loop refrigeration system, a dual-flow transfer coupling, a conduction-cooling scheme, and an internal composite torque tube configuration. Based upon these objectives, a motor was design, built and successfully tested at rated speed and at greater than its rated power. This paper provides an overview of the design of the motor and discusses the results of a series of tests which were performed on the motor.

This work was supported in part by the US Department of Energy under its Superconductivity Partnership Initiative Award DE-FC36-93CH10580.

* Rockwell Automation, 26391 Curtiss Wright Pkwy, Suite 102, Richmond Heights, OH 44143.

II. Design of the 1000-hp Motor

A. Overview

As shown in Fig. 1, the 1000-hp HTS motor has superconducting coils mounted on the rotor, cooled by gaseous helium to cryogenic temperature (on the order of 30°K). The gaseous helium is supplied to the rotor via a rotating transfer coupling. The rotor cold space is insulated from the ambient by a vacuum space. Torque is transmitted through the vacuum space via composite torque tube extensions that connect the cold space to the motor shaft.

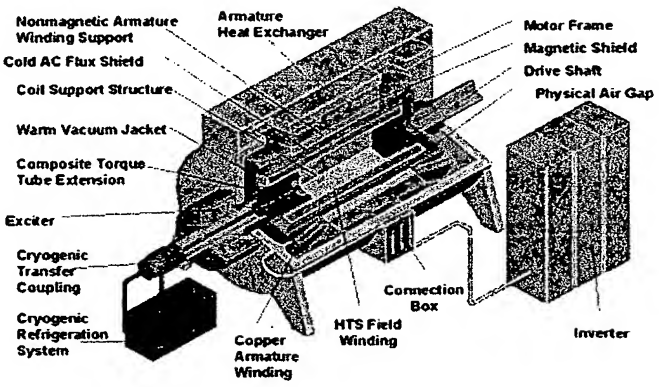

Fig. 1. Schematic of the 1000-hp HTS motor system.

The motor stator consists of an air-core winding surrounded by a magnetic core. The armature winding consists of relatively conventional water-cooled coils wound from Litz wire and supported in a non-magnetic slotted cylindrical structure. This winding is inserted into a cylindrical stack of laminations of electrical steel which forms the stator flux return path.

The design parameters for the 1,000-hp HTS motor are summarized in Table I. The motor efficiency in this table accounts for the input power of the cryogenic refrigeration system.

The 1000-hp HTS motor enclosure has an axial cross section of 1.17 m x 1.17 m and is 1.45 m in length while that of a

TABLE I
MOTOR DESIGN PARAMETERS

Motor Rating	1,000 hp
Motor Speed	1,800 rpm
Rated Armature Terminal Voltage	4,160 V
Rated Frequency	60 Hz
Rated Armature Line Current	106 A
Number of Poles	4
Power Factor	1.0
Efficiency	97.1%
Armature O.D.	0.686 m
Armature Length	1.22 m
Field-Winding Operating Temperature	33 K
Field Winding Current	120 A
Rotor O.D.	0.4 m

conventional motor of comparable rating and efficiency has an axial cross section of 1.5 m x 1.5 m and a length of 1.5 m. The specific weight of this motor stands at 6 lb/hp at 1,000 hp, compared to 6.7 lb/hp for its conventional counterpart. Figure 2 is a photograph of the completed 1000-hp HTS motor.

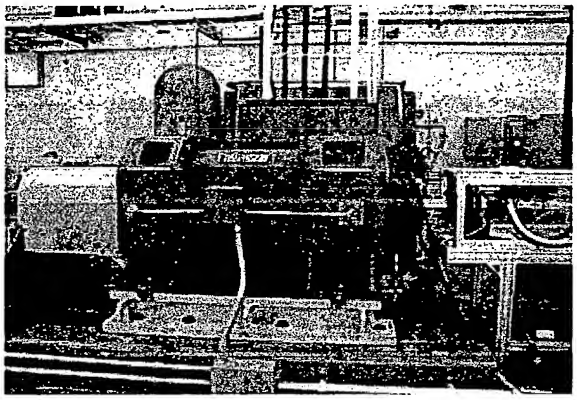

Fig. 2. The 1000-hp HTS motor.

B. Rotor Structure

The major components of the rotor include a main support structure for the HTS field winding coils, two torque tubes, an AC flux shield, a vacuum enclosure, and two sets of end shaft and flange assemblies. A photo of the rotor, before installation of the AC flux shield or vacuum enclosure, is shown in Fig. 3.

The HTS coils are bolted onto the rotor support structure and covered by a cold AC flux shield to minimize AC fields at the coils during motor transients. To minimize the heat-leak component of the refrigeration load, the cold mass of the rotor cryostat is thermally insulated by a combination of vacuum space and multi-layer insulation. The outer vacuum jacket of the rotor cryostat remains warm during normal operation and hence the cold mass of the rotor shrinks as it is cooled. This thermal differential is compensated for by a pair of diaphragms at the ends of the rotor cryostat. These diaphragms also serve as part of the vacuum enclosure of the rotor cryostat and were designed to withstand the load due to the pressure differential between the external ambient environment and the internal vacuum space in the rotor cryostat.

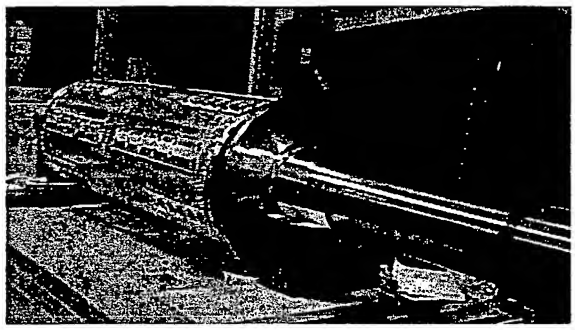

Fig. 3. Rotor of the 1000-hp HTS motor.

The main rotor-support structure is made of the same aluminum alloy as the HTS field-coil mandrel. It is shrink-fitted over a stainless steel structure into which helical grooves were cut to accommodate the heat exchanger cooling tubes. Thermal communication between the main structure and the HTS coils is through conduction.

The main rotor structure is supported by two fiberglass/epoxy composite torque tubes [3]. In addition to transmitting torque, the torque tubes provide a low-thermally-conducting bridge for the space between the rotor cryostat and the warm ambient environment. The low thermal conductivity of the composite material limits the parasitic heat leak through both torque tubes. To insure the mechanical integrity of the motor, the torque tubes were designed to withstand a three-phase short circuit fault on the motor, a scenario in which the amplitude of the fault torque can reach 16 times the rated nominal value. Metal fittings are attached to both ends of each composite torque tube. At each end of the rotor, these metal fittings are mechanically fastened to the main structure at the cold end and to the end shaft and flange assembly at the warm end. Extensive testing was carried out on the torque-tube assemblies to verify their strength and fatigue characteristics prior to their application to the 1000-hp motor.

An AC flux shield covers the HTS field winding coils. It is secured at both ends to the flanges of the cold mass in order to insure that it can withstand transient torques associated with fault conditions. This shield operates at cryogenic temperatures and therefore is referred to as a cold flux shield.

As a prototype, the rotor cryostat, including the field winding coils of the 1,000-hp HTS motor, is instrumented to monitor the performance the rotor components. Signals from the sensors are transmitted from the rotating frame of the rotor to the stationary environment through an optical telemetry system and then logged by a data acquisition system.

Another key element of the HTS motor system is the rotating transfer coupling which connects the cryogenic refrigerator to the rotor cryostat of the HTS motor and provides a passage for helium gas to enter and return from the rotor cryostat. A rotating seal is required to complete the transition from the stationary cryogenic refrigeration system to the rotating rotor cryostat. A combination of ferro-fluidic and mechanical seals is used. Extensive testing on the prototype transfer coupling was carried out, both for its dynamic behavior and thermal

performance.

C. Superconducting field winding

The HTS field winding consists of four coils wound with a multi-filament BSCCO (Bismuth, Strontium, Calcium, Copper Oxide) tape conductor. Each coil consists of a stacked set of racetrack-shaped coils encased in an aluminum alloy structure. The overall length of HTS wire required for the field winding measures approximately 18 km. Various field-winding parameters are found in Table II. For the tests described in this paper, field current was supplied to the field winding from a stationary dc field supply through a brush/slip-ring system.

TABLE II
FIELD-WINDING PARAMETERS

Operating temperature	33 (°K)
Turns/pole	1220
Rated current	120 A
Amp-turns/pole	146,400

D. Stator

The armature winding of the 1,000-hp HTS motor was designed for ambient-temperature operation. It is constructed from 48 form-wound coils. Because this is an air-core machine and hence the armature coils operate in the full magnetic flux of the motor, they are wound from Litz wire in order to reduce eddy-current losses. The coils are supported by a G-10 lamination stack (with teeth much like those in a conventional machine) which, in turn, is inserted in a laminated-steel cylindrical core. The air-core armature configuration was chosen to reduce iron losses which would occur due to the high magnetic flux densities created by the HTS field winding.

Both the armature winding and the motor frame are water-cooled by embedded cooling tubes. By permitting an increase in armature cooling capability, water cooling helps to reduce the size of a motor for a given rating. In addition, the auxiliary power requirement for water cooling is less than that for air cooling and hence this choice contributes to improved motor efficiency.

A single-path water cooling circuit is embedded in the stator frame. A more elaborate scheme is employed for the stator winding cooling. Each of the forty-eight stator coils is wound with eight turns of a single piece cooling tube. The heavy nylon varnish insulation on the individual strands of the Litz wire bundle in combination with the turn insulation between Litz wire conductor and cooling tube provide sufficient insulation between the cooling tube and stator winding wire. All of the stator coils are cooled in parallel, with cooling tubes from each coil connected to a pair of supply and return manifolds.

E. Cryogenic cooling system

In contrast to previous demonstrations where open-loop (once-through) refrigeration systems were used, the 1000-hp HTS motor includes a closed-loop refrigeration system. Cold helium gas is supplied to the rotor through a rotating transfer system which also extracts the warm gas and returns it to the cryogenic refrigeration system to be re-cooled. This is a significant accomplishment of this project, since a closed-loop system is a requirement for any commercially-viable HTS motor system.

Based upon the operating characteristics of the HTS conductor used in this machine, the operating temperature of the HTS field winding was selected to be 33°K (-400°F). The commercially-available helium refrigerator chosen for this motor has a capacity sufficient to keep the rotor temperature at or below 20°K for a rotor heat rate of up to 145 W. This is a few times larger than is required for the 1000-hp HTS motor. A pair of cryogenic bayonets in the rotating transfer coupling allows quick connection between the motor and the helium refrigerator. Once inside the rotor, the helium gas is circulated through a heat-exchanger cooling loop in the coil support structure where it picks up thermal energy from the rotor (internal dissipation and heat from any heat leak) before returning to the helium refrigerator.

III. INSTRUMENTATION AND TEST SETUP

The 1000-hp HTS motor was mounted on a test stand and connected to a 2,500-hp conventional AC motor. This AC motor was in turn connected to the local power grid through an inverter. It could therefore be used as a drive motor to spin the HTS motor for open-circuit testing as well as a load, with load power being regenerated back to the local power grid. A photo of this arrangement is shown in Fig. 4 in which the HTS motor is coupled to the load motor by a torque transducer. Neither the inverter for the load motor or the inverter for the 1000-hp HTS motor can be seen in this figure. Not readily seen in Fig. 4 is the reverse Brayton refrigerator which was used for this series of tests. The refrigerator delivered helium gas at a temperature of around 30°K to the rotor[1].

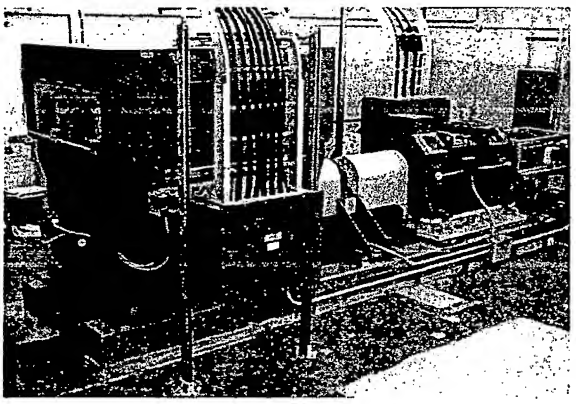

Fig. 4. Test setup for the 1000-hp HTS motor. The 2500 hp conventional AC load motor in seen in the foreground at the left of the photo with the much smaller 1000-hp HTS motor seen at the right of the photo.

The 1000-hp HTS motor was tested both at rated speed connected to the 60-Hz power grid and also as a variable-speed motor operated from a variable-speed current-source-

[1] Although the refrigerator used for this test was capable of cooling the rotor to significantly lower temperatures, this was not done in order to accurately simulate the as-designed operation of the HTS motor

inverter drive system. Figure 5 shows the 1250-hp Allen-Bradley inverter.

Fig. 5. 1250-hp Allen-Bradley inverter

The mechanical shaft power of the HTS motor was determined by torque and speed measurement. Torque was measured using a 50,000-in.-lb. torque transducer that was used to couple the HTS and load motors. The motor speed was measured using a shaft-mounted tachometer that also supplied a speed signal to the load-motor drive. Voltage, current, and power for all three phases of the HTS motor were measured. Calculation of motor efficiency was based upon time-averaged input and output power measurements obtained over a two-minute period.

During construction of the motor, cryogenic temperature sensors were mounted at a number of locations within the rotor cryostat for the purpose of monitoring the operating condition of the superconducting coils. Readings from these sensors were transmitted from the rotating frame of the rotor to the stationary environment via an optical telemetry system. A significant advantage of this system is its immunity to the various sources of electromagnetic noise that tend to occur when testing such large motors. An array of LEDs on the rotating side transmit data to a set of stationary phototransistor. A photo showing the major components of the optical telemetry system is seen in Fig. 6. Clearly visible in this photo is a rotating disc which holds the rotor LEDs and which also includes the secondary winding of a rotating transformer which supplies power to the rotating system. The photo-transistors are mounted on a stationary support plate which can be seen in the foreground of the photo.

All of the data collected during the various tests was collected by a computerized data acquisition system and saved for later analysis.

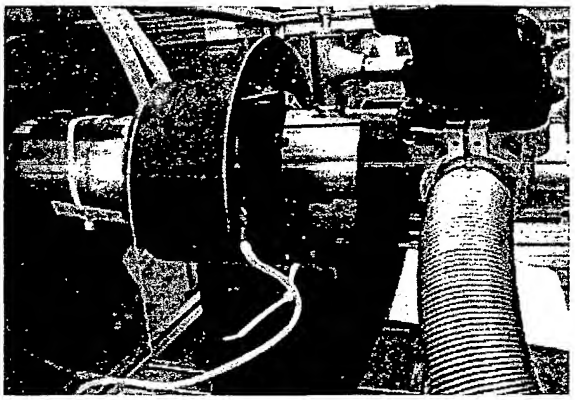

Fig. 6. Optical telemetry system.

IV. Testing of the 1000-hp Motor

A. Cool down

Figure 7 shows a plot of the coil temperature versus time during a typical rotor cool down. Cool down took place while the rotor was stationary. This cool down transient clearly indicates an important characteristic of a well-design HTS motor. The motor design requires that rotor losses and heat leak into the rotor must be extremely low under normal operating conditions and hence only a relatively small refrigerator is required to maintain normal operating conditions. This is of course important in insuring a high-efficiency motor. From Fig. 7 we see that one consequence is that, because of its small rating, it takes a very long time (on the order of 36 hours) for this small refrigerator to cool the rotor from ambient temperature to its operating temperature of 33°K[2].

B. No-load tests

For these tests, the rotor was cooled to its design operating temperature of 33°K and the load motor was used to drive the 1000-hp HTS motor to its rated speed of 1800 rpm.

[2]As discussed in Sect. II-E, the refrigerator used in this experiment is actually over-rated for this machine and the cool-down time using a properly rated refrigeration system would have been even longer than that shown here.

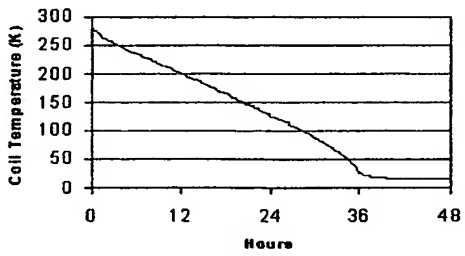

Fig. 7. Plot of coil temperature versus time during a typical cool down.

An open-circuit test was conducted by applying excitation current to the field winding and measuring the resultant line-to-line open-circuit armature voltage. Because of the large air-gap of this machine, the resultant data is linear with a slope 36.1 Vrms (line-line) per Ampere of field current. This result is approximately 3.5% higher than the value predicted during the design phase, a result which can be attributed to the fact that end-region flux causes additional coupling to the stator winding that was not accounted for in the design analysis.

Based upon this result, the field current corresponding to a rated open-circuit voltage of 4,160 V can be calculated as

$$\text{AFNL} = 115.2 \text{ A} \tag{1}$$

A short-circuit test was conducted by applying a three-phase short circuit to the armature winding and measuring the phase current as a function of field current. The resultant data is linear with a slope of 5.47 Arms per Ampere of field current. Assuming a motor base power of 1000 hp = 746 kW, the base armature current of the motor can be calculated as

$$I_{\text{a,base}} = \frac{746 \times 10^3}{\sqrt{3}\ 4160} = 103.5 \text{ Arms} \tag{2}$$

The field current corresponding to rated short-circuit current is thus

$$\text{AFSC} = 18.9 \text{ A} \tag{3}$$

and hence the motor per-unit synchronous reactance can be calculated as

$$X_s = \frac{\text{AFSC}}{\text{AFNL}} = 0.16 \text{ pu} \tag{4}$$

With the HTS motor driven at its rated speed by the load motor, rotational losses were directly measured using the in-shaft torque transducer. By operating the motor without field excitation, the friction and windage losses were determined to be approximately 1.4 kW. This value is an average of measurements which had a variation of around 0.3 kW which is reasonable given the resolution of the test instrumentation.

The machine was then excited to rated voltage and the losses increased to 14.7 kW (an averaged value of measurements with a variation of around 1.0 kW). The additional increment of 13.3 kW can be attributed to losses in the iron core as well as to eddy-current loss in the armature winding.

The 13.3 kW of core and armature eddy-current loss is higher than was expected from design calculations. Extensive analysis of the test data indicated that this additional loss can be attributed in great measure to higher-than-expected losses induced in the end regions of the stator core (back-iron laminations) by end-region flux produced by the rotor winding.

Short-circuit losses were calculated based upon a measured value of the armature phase resistance of $R_a = 0.224\ \Omega$. Based upon the rated armature current of $I_a = 103.5$ A, the short-circuit loss is then

$$P_{sc} = 3I_a^2 R_a = 7.2 \text{ kW} \tag{5}$$

C. Full-load tests

The HTS motor was tested at an output power of 1000-hp at 1800 rpm when connected directly to the local 60-Hz power system at 4160 V. This test, of approximately 3 hours duration, was sufficiently long to achieve thermal equilibrium in the rotor. The measured motor efficiency under this operating condition (determined as the ratio of measured shaft output power to measured electrical input power) was approximately 96.7%[3], corresponding to a full-load loss of approximately 25.5 kW.

The full-load losses can be approximated as the sum of the open-circuit losses (P_{oc} = 14.7 kW) and the short-circuit losses. Thus, the estimated full-load loss is $P_{fl} = P_{oc} + P_{sc}$ = 21.9 kW. The 3.6 kW difference between this and the full-load loss determined from the measured full-load efficiency is well within the measurement tolerances of the various instruments used in this test; as instrumented for the full-load tests, the test-stand torque transducer was rated at 1300-hp and the electric power meter was set to 3 MW full-scale.

Extensive testing was performed on the HTS motor, including a test during which the motor was loaded to an output power of 1600 hp. This test was of brief duration and not sufficiently long to achieve thermal equilibrium in the motor.

All of the load tests described above were performed with the HTS motor operating at constant speed connected to a 60-Hz sinusoidal system. For a motor intended for variable-speed operation, such tests are idealized in the sense that the applied stator phase voltages are relatively harmonic-free.

The 1000-hp HTS motor was designed for variable-speed operation. A series of tests were performed using the 1250-hp inverter shown in Fig. 5. These tests showed an increase in rotor loss over that observed during the 60-Hz sine-wave tests. The likely source of the additional losses are asynchronous magnetic fields created by time-harmonic currents produced by the variable-speed drive. An increase in rotor losses is not uncommon in conventional machines when powered by a variable-speed drive. However, for a superconducting motor, rotor loss is particularly troublesome since it acts to increase the temperature of the rotor cold space and hence requires additional cooling power to keep the superconducting field coil at its desired operating temperature. An increase in cooling power will reduce the overall efficiency of the motor, since cooling power is an additional loss in the superconducting-motor system.

Both of these consequences of increase rotor loss have a significant impact on superconducting-motor performance. Based upon the tests performed, it was concluded that motor/drive interaction studies are key to obtaining acceptable performance of a variable-speed superconducting motor system. Coordinated design of the inverter, inverter control, rotor shields and rotor-cooling methods are required. System studies to investigate motor and drive design modifications are now being conducted, as a continuation of this project, with the objective

[3]Note that the measured efficiency of 96.7% does not account for the input power to the refrigerator, which clearly should be charged against the efficiency of the HTS motor. However, the refrigerator used in this experiment was sufficiently oversized that it was not possible to get a reasonable estimate of the refrigeration power which should rightfully be charged in this case.

of obtaining optimal variable-speed drive performance for large HTS motors.

V. Conclusion

A 1000-hp superconducting motor with an HTS field winding was designed, built and succesfully tested to its rated load. The goal of this motor demonstration, based upon available HTS wire performance, was to achieve performance levels comparable to those of similarly-rated conventional motors. This goal was achieved. The program provided a key milestone in superconducting-motor development by demonstrating the technical viability of the HTS large-motor concept. HTS motors can be expected to become commercially viable at power levels where their efficiency exceeds that of conventional motors. The results of this program will be invaluable in the design of such "next-generation" HTS motors.

This program met or exceeded all of its goals and provided operational verification of a number of new novel system technologies. In addition, it provided significant insight into additional challenges which must be addressed in future HTS motors, including the need to develop techniques for the reduction of core-end losses and the need for further study of the interaction between HTS machines and power inverters in variable-speed applications.

Acknowledgment

This program was funded in part by the U.S. Department of Energy through a Superconductivity Partnership Initiative program under cooperative agreement DE-FC36-93CH10580 with the Reliance Electric Company. The authors wish to acknowledge the valuable contributions of the participating team members in this program; Reliance Electric Company, American Superconductor Corporation, Sandia National Laboratories, Centerior Energy Corporation and the Electric Power Research Institute.

References

[1] Jordan, H., Feasibility Study of Electric Motors Constructed with High Temperature Superconducting Materials, Electric Machines and Power Systems, 16:15-23 (1989).

[2] Schiferl, R., et al., High Temperature Superconducting Synchronous Motor Design and Test, Proc. of the American Power Conference, Chicago, IL (1996).

[3] Shoykhet, B., Design of Composite Torque Tubes for High Temperature Superconducting Motors, 3rd U.S. Navy Symposium on Electrical Machines, Philadelphia, 2000.

Viatcheslav Dombrovski Viatcheslav Dombrovski began his engineering and scientific career with Electrosila Ltd. in St. Petersburg, Russia where he held a number of design and research positions and also served as a university professor. He joined Reliance Electric in 1997 and currently holds the title of Engineering Scientist in the Rockwell Automation Advanced Technology group in Cleveland, Ohio. His current research activities include the design of wide variety of motors; HTS, induction, permanent-magnet, and high-speed switched-reluctance motors as well as magnetic couplings. Dr. Dombrovski received his BS, SM, Ph.D, Dr.Sc degrees and professor's diploma in Electrical Engineering from the Technical University in St. Petersburg, Russia. He is the author of more than 100 papers, 6 books on electric machinery theory, design and production and has been awarded 35 patents. His special field of interest includes superconductivity and its application to electric machinery.

David Driscoll David Driscoll received his B.S. degree in engineering from Idaho State University in 1980, the M.S. and Ph.D. degrees were received in mechanical engineering from Purdue University in 1986 and 1991, respectively. He is currently employed by Rockwell Automation as the manager of the Advanced Technology Lab in Cleveland, OH.

Boris Shoykhet Boris A. Shoykhet was born in Leningrad, USSR, on September 11,1946. He graduated from the School of Mathematics and Mechanics of Leningrad State University in 1969, and received his Ph.D in Mathematical Physics from Mathematical Institute of Academy of Science of USSR in 1975. His employment experience included 19 years at the Institute of Hydraulic Engineering, Laboratory of Structural Mechanics, Leningrad, USSR, 2 years at LORD Corp, Composite Product Development, Erie, PA , and 12 years at Reliance Electric/Rockwell Automation, Cleveland, OH, in the Superconducting Motor Group. He has published over 50 papers and a monograph, and holds 8 patents in the area of the superconducting electrical machinery. He received the Distinguished Paper Award from International Journal of Engineering Science in 1999 and the Rockwell Automation Engineer of the Year Award in 2001.

Stephen Umans Stephen D. Umans was born in Cleveland, Ohio on November 10, 1948. He is a graduate of the Massachusetts Institute of Technology, having received the S.B. and S.M. (1972) and Sc.D. (1976) degrees, all in electrical engineering. Dr. Umans most recently held the position of Principal Research Engineer in the Electromechanical Systems Laboratory and the Electrical Engineering and Computer Science Department at MIT. He is currently working as an independent consultant, with specific focus in the areas of electromechanics, electric power systems and both macro- and micro-scale electric machinery. Dr. Umans is co-author of the textbook ELECTRIC MACHINERY, published by McGraw-Hill, and is a Fellow of the IEEE.

Joe Zevchek Joseph K. Zevchek is a Senior Research Engineer, serving in the capacity of Test Engineer, in Rockwell Automation's Advanced Technology department. He graduated from Cleveland State University with a Bachelor of Science degree in physics. Joe Zevchek has worked for Reliance Electric, now Rockwell Automation, since 1989 and has been involved with superconducting motor research since 1994.

CONSTRUCTION AND TESTING OF A 1,000 HP HIGH-TEMPERATURE SUPERCONDUCTING MOTOR

Paper No. PCIC-2002-28

Burt Zhang, Ph.D.
Rockwell Automation
24800 Tungsten Road
Cleveland, OH 44117
USA

David Driscoll, Ph.D.
Rockwell Automation
24800 Tungsten Road
Cleveland, OH 44117
USA

Viatcheslav Dombrovski, Ph.D.
Member, IEEE
Rockwell Automation
24800 Tungsten Road
Cleveland, OH 44117
USA

Abstract - An air-core, synchronous motor with a high temperature superconducting field winding has been successfully constructed and tested. The motor features a salient-pole superconducting field winding that operates at a nominal temperature of *30 K*. A closed-loop (reverse Brayton cycle) cryogenic refrigeration system is used for initial cool-down and normal operation. Designed for *1,000 hp*, this motor was demonstrated at *1,600 hp* during operation at its rated speed of *1,800* rpm. This work summarizes the design objectives and requirements, technical challenges, data acquisition techniques and testing results.

I. INTRODUCTION

The development effort for super-efficient electric motors started in 1987, shortly after the discovery of high-temperature superconducting (HTS) materials in 1986. The higher operating temperature of the HTS materials, compared to previous superconductors that required liquid helium cooling at *4.2 K*, results in lower cooling costs to maintain the coils in their superconducting state. For superconducting rotating machinery, the lower cooling costs provide the potential to reduce the rating of economically viable products from the hundreds of megawatt range of central station generators to the thousands of horsepower range of large electric motors. It has been estimated that superconducting motors offer benefits in terms of a reduction of *50%* in both losses and size compared to conventional motors of the same rating [1].

The expected benefits of HTS motors are higher motor efficiency and smaller motor size. Both of these benefits are a direct result of being able to use the HTS motor field winding to create a high magnetic field thereby reducing the motor size [2]. The smaller motor size reduces friction and windage, and the amount of losses in the armature materials (copper and steel). Commercial HTS motors are expected to have about half of losses of conventional high-efficiency motors of the same rating, taking into account the input power required for the HTS winding cooling system. The intended application of superconducting motors is mainly targeted at driving pumps, fans, and compressors for utility and industrial environments where continuous operation and minimal maintenance are expected.

The goal of the *1,000-hp* HTS motor development is to demonstrate an HTS motor comparable with conventional motors in terms of efficiency and size for the same power rating. Features of significance associated with this motor demonstration include a closed-loop refrigeration system, a dual-flow transfer coupling, a conduction-cooling scheme, and an internal composite torque tube configuration. This four-pole motor is strategically designed for operation from an adjustable-speed drive (ASD), although an alternative design has been completed to allow across-the-line starting. As shown in Fig. 1, a typical HTS motor has superconducting coils mounted on the rotor, cooled by cryogen at cryogenic temperature. The cryogen is supplied to the rotor via a rotating cryogenic transfer coupling. The cold space of the rotor cryostat, an apparatus containing cryogenic environment, is insulated from the ambient by a vacuum space. Torque is transmitted through the vacuum space via torque tube extensions that connect the cold space to the motor shaft. The stator winding is a copper winding supported by a nonmagnetic and nonconductive core. Outside of this core is a laminated steel frame and flux shield that provides the return flux path for magnetic fields created by the HTS and armature windings. This frame can be constructed from magnetic steel lamination material used in conventional motors. All materials inside of this frame will be nonmagnetic (relative permeability equal to one) so that the distribution of magnetic field will be as if in air. For this reason, the motor is called an air core synchronous motor.

The primary design parameters and performance characteristics for the *1,000-hp* HTS motor are summarized in Table I. The design motor efficiency takes into account the cryogenic refrigeration system input power.

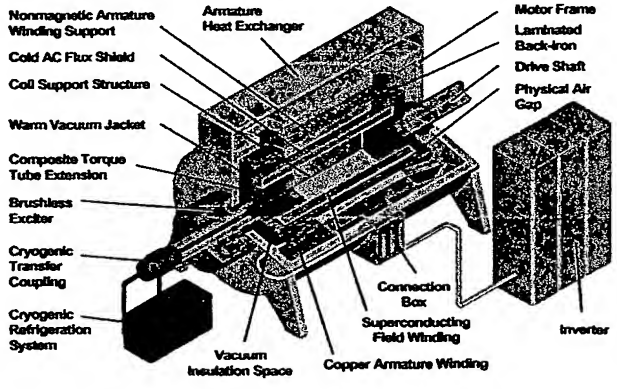

Figure 1. Schematic of HTS motor system.

TABLE I
MOTOR DESIGN PARAMETERS

Motor Rating	1,000 hp
Motor Speed	1,800 rpm
Number of Poles	4
Rated Armature Terminal Voltage	4,160 V
Rated Armature Line Current	106 A
Power Factor	1.0
Motor Design Efficiency	97.1 %
Armature O.D.	0.686 m
Armature Length	1.22 m
Field Winding Operating Temperature	33 K
Field Winding Current	120 A
Max. Field Winding Flux Density	1.5 T
Rotor O.D.	0.4 m

Dimensions of the motor enclosure measure at 1.17 m × 1.17 m × 1.45 m, which compare favorably to that for a conventional motor of comparable rating and efficiency at 1.5 m × 1.5 m × 1.5 m. In addition, the specific weight of this motor stands at 6 lb./hp at 1,000 hp, compared to 6.7 lb./hp for its conventional counterpart.

The development involves a collaboration of six team members from industry, utility companies and government laboratories. This work is supported in part by the Department of Energy under its Superconductivity Partnership Initiative Award DE-FC36-93CH10580

II. COOLING SYSTEM

Compared to previous demonstrations, where open-loop (once-through) systems had been used for cooling the HTS field winding coils, the use of a closed-loop refrigeration system is considered a major step toward commercialization of HTS motor and an essential feature of a commercially viable HTS motor system. The system to be used for initial component and system testing is a recuperative type and runs in a reverse Brayton cycle. Development for advanced close-loop systems is underway with the objective focused on improvement of system reliability and substantial reduction of system costs and size. Cryocooler selection criteria and cycle options are discussed in more details elsewhere [3].

The operating environment of the HTS field winding coils is based on current HTS conductor technology and is set at *33 K (- 400 °F)* with a future potential of running at higher temperatures. In order to produce the required refrigeration and deliver it to the HTS coils residing in the rotor cryostat, a closed-loop cryogenic refrigeration system is needed. The selected helium refrigerator is commercially available and has a capacity of *145 W* on a *20 K* return, which is a few times higher than needed for the *1,000-hp* HTS motor. Helium gas is delivered to the rotor cryostat by a pair of vacuum-jacketed transfer lines through a rotating transfer coupling. A pair of cryogenic bayonets allows quick connection between the helium refrigerator and rotor cryostat. Once inside, the helium gas is circulated in a heat exchanger cooling loop in the coil support structure where it picks up the parasitic heat leak before returning to the helium refrigerator.

III. SUPERCONDUCTING COILS

The HTS field winding consists of four coils wound with a tape multifilament BSCCO (Bismuth, Strontium, Calcium, Copper Oxide) conductor. Each coil consists of a stacked set of racetrack shaped coils encased in an aluminum alloy structure. The overall length of HTS wire required for the field winding measures approximately *18 km*. Performance requirements for the coils are listed in Table II.

TABLE II
FIELD WINDING REQUIREMENTS

Amp-turns/pole	146,400
Temperature (K)	33
Full coil turns	1220
Current (amp)	120

IV. ROTOR STRUCTURE

The major components of the rotor cryostat include a main structure that supports the HTS field winding coils, two torque tubes, an AC flux shield, a vacuum enclosure, and two sets of end shaft and flange assemblies. A photo of the rotor is shown in Fig 2 without the AC flux shield or vacuum enclosure.

In the rotor, the HTS coils are bolted on a support structure and covered by a cold AC flux shield to minimize the AC fields on the coils during motor transients. These coils can be exchanged or replaced once the vacuum jacket is removed. The cold mass of the rotor cryostat is thermally insulated by a combination of vacuum space and multi-layer insulation (MLI) to minimize refrigeration load when the system is energized. The outer vacuum jacket of the rotor cryostat remains warm during normal operation while the cold mass of the rotor cryostat shrinks. This thermal movement differential is compensated by a pair of diaphragms at the ends of the rotor cryostat. These diaphragms also serve as part of the vacuum enclosure of the rotor cryostat. The DC power supply to the HTS field winding is delivered by slip rings mounted on the non-drive end shaft. In a parallel effort, a brushless exciter has been developed for the delivery of DC power and will be later integrated with the motor system.

The HTS field winding coils are secured to the main structure made of the same aluminum alloy as the coil mandrels. It is shrink-fitted over a stainless steel structure where helical grooves were cut to accommodate the heat exchanger cooling tubes. Cryogenic refrigeration carried by cold helium gas is delivered to the cold mass of the rotor cryostat by a feed-line tube. The coolant within the heat exchanger then intercepts the heat leak in the main structure. The thermal communication between the main structure and the HTS coils is through conduction.

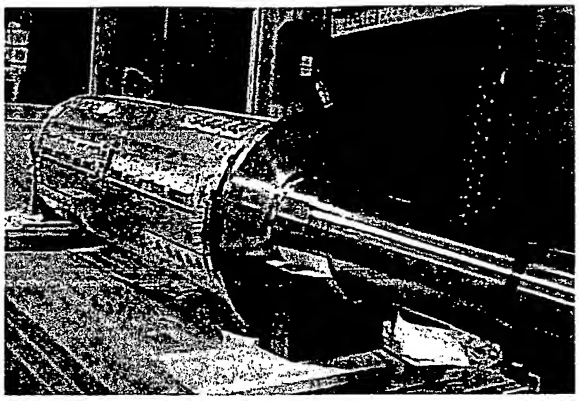

Figure 2. Rotor structure of *1,000 hp* HTS motor.

The main structure is supported by two composite torque tubes with one at each end [4]. The torque tubes bridge the cold space of the rotor cryostat and the warm ambient environment, in addition to transmitting the torque. Each torque tube experiences the large temperature difference between the cold mass of the rotor cryostat and the warm end shaft. The low thermal conductivity of the composite material limits the parasitic heat leak through both torque tubes. As the most critical structural component, the torque tubes are designed to withstand a three-phase short circuit fault on the motor, a scenario where the amplitude of the fault torque could reach 16 times the rated nominal value. A fiberglass epoxy composite was chosen as the torque tube construction material to reduce parasitic heat leak through conduction. Metal fittings are attached to both ends of each composite torque tube. At each end of the rotor, the metal fittings of the torque tube are mechanically fastened to the main structure at the cold end and to the end shaft and flange assembly at the warm end. Extensive testing has been carried out on torque tube assemblies to verify their strength and fatigue characteristics.

An AC flux shield covers the HTS field winding coils. It is secured at both ends to the flanges of the cold mass in order to withstand the oscillating transient torque in fault conditions. This shield operates at cryogenic temperatures and therefore is referred to as cold flux shield. Both end flanges for the rotor shafts serve as diaphragms to take up the thermal movement differential between the cold mass and the vacuum jacket of the rotor cryostat. The diaphragms were optimized by finite element analysis (FEA), which resulted in a properly contoured element that deflects when the thermal differential movement occurs during motor operation. They are also designed to withstand the load due to a pressure differential between the external ambient environment and the internal vacuum space in the rotor cryostat.

As a prototype, the rotor cryostat, including the field winding coils of this *1,000-hp* HTS motor, is equipped with cryogenic instrumentation for monitoring the performance of the system. Signals from the sensors are transmitted from the rotating frame of the rotor to the stationary environment through an optical telemetry system and then logged by a data acquisition system (DAQ).

Another key element of the HTS motor system is the rotating cryogenic transfer coupling. The transfer coupling links the cryogenic refrigerator to the rotor cryostat of the HTS motor and provides a passage for helium gas to enter and return from the rotor cryostat. A rotating seal is required to complete the transition from the stationary cryogenic refrigeration system to the rotating rotor cryostat. A combination of ferrofluidic and mechanical seals is used in the present design. Extensive testing on the prototype transfer coupling was carried out for its dynamic behavior and thermal performance. An alternative design for the transfer coupling has also been completed, which substantially reduces the structural complexity with expected improvement on reliability. The alternative design has also been constructed and tested. It has been designated for use in the *1,000-hp* HTS motor system in conjunction with a newly constructed reverse Brayton cycle helium refrigerator.

V. Stator Development

The 1,000-hp HTS motor features forty-eight slots and forty-eight form-wound stator coils, which represent a so-called two-layer type winding. The stator winding is made of copper conductor operating at ambient temperatures. Twisted Litz wire bundles are used for reduction of eddy current losses.

The coils are supported by a G-10 lamination stack, which fits within a steel laminated back iron. The design objective is to take advantage of the HTS rotor field winding, in order to increase the motor efficiency and decrease the volume. The air-core armature type was chosen to reduce losses because the high magnetic field created by the HTS field winding saturates the steel laminations. Both the stator winding and frame are water-cooled with embedded cooling tubes. This approach enhances the cooling effectiveness and offers the potential of running the HTS motor at a power rating higher than the design nominal. It allows significant increase in line current which is the primary driving parameter for reduction of motor volume. At the same time, the auxiliary power required for cooling is much smaller compared to that for an air-cooled stator, which also increases the motor efficiency. Such effects will become much more pronounced on the *5,000-hp* HTS motor to be developed in the near future.

A single-path water cooling circuit is embedded in the stator frame. A more elaborate scheme is deployed for the stator winding cooling. Each of the forty-eight stator coils is wound with eight turns of a single piece cooling tube. The heavy nylon varnish insulation on the individual strands of the Litz wire bundle, and the turn insulation between Litz wire conductor and cooling tube, provide sufficient insulation against a short circuit between the cooling tube and stator winding wire. On the other hand, good thermal contact between the cooling tubes and stator winding is established through the vacuum pressure impregnation (VPI) process. All stator coils are cooled in a parallel circuit with cooling tubes from each coil connected to a pair of supply and return manifolds.

VI. MOTOR TESTING

The HTS motor was mounted on a test bed and loaded up by a *2,500-hp* conventional AC motor. A reverse Brayton refrigerator was used for the cooldown and normal operation of the superconducting field winding coils. The refrigerator delivered helium gas at temperatures around *30 K* to the rotor cryostat through a transfer coupling. A photo of this arrangement is shown in Fig. 3 where the HTS motor is coupled to the load motor by a torque transducer.

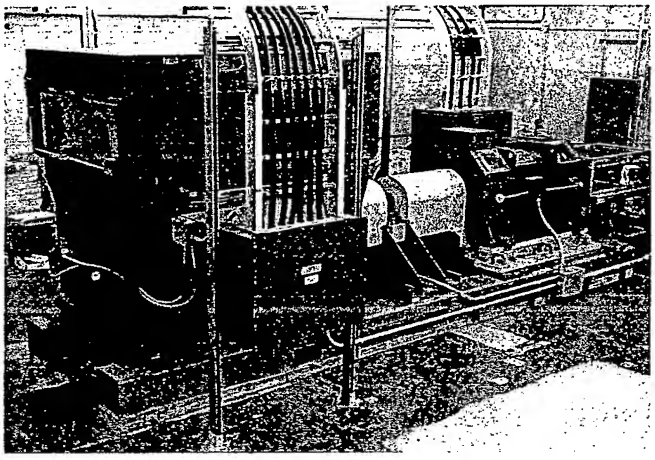

Figure 3. Setup for HTS motor testing (2500 hp conventional AC load motor in foreground, HTS motor in background).

The mechanical energy produced by the HTS motor is converted to electrical energy through the load motor and a regenerative drive. The load motor works as a generator and the drive serves as an interface to sequence the power back to the lines. This regenerative scheme reduces the power consumption during motor testing to system losses, instead of the rated motor power.

The output power of the HTS motor is determined by torque and speed measurement. A *50,000-lb. in.* torque transducer that couples the HTS and load motors provides the torque information in terms of a DC voltage output. The motor speed is recorded by a tachometer. This piece of information is also fed back to the load motor drive for speed regulation.

Voltage, current, and power factor for all three phases of input power to the HTS motor are monitored. Calculation of motor efficiency is time-averaged from input and output power over a two-minute period. All motor information is collected by a computerized data acquisition system (DAQ) and saved for analysis.

Cryogenic temperature sensors are mounted within the rotor cryostat for monitoring the operating condition of the superconducting coils. Readings from these sensors are transmitted from the rotating frame of the rotor to the stationary environment via an optical telemetry system.

A significant advantage in using such a system is its immunity to electrical and magnetic noises in the motor test area. An array of LED's on the rotating side emit signals to be received by a group stationary phototransistors that compose the optical receiver. A photo depicting the optical telemetry system is shown in Fig. 4 where a rotating disc carrying the LED's and the stationary frame of the optical receiver are visible.

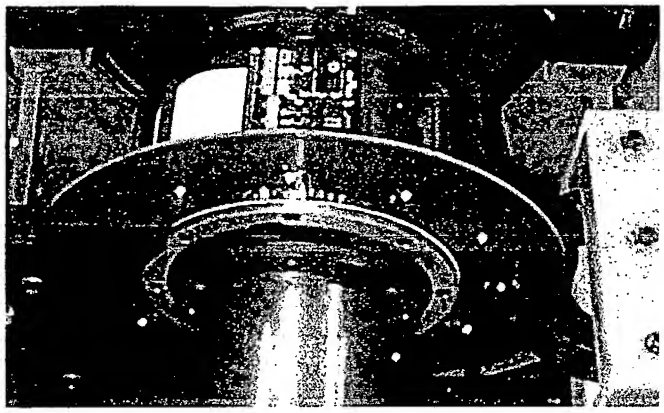

Figure 4. Optical telemetry system.

Testing of the motor followed NEMA standards, taking into account special features of the HTS motor. Primary aspects of the testing can be summarized as follows:

A. insulation resistance / hi-pot
B. Ohm resistance of stator winding
C. phase sequence
D. no-load test
E. short-circuit test
F. rotor impedance (stationary)
G. thermal performance
H. motor efficiency (no-load / load)
I. Load tests
J. Inverter operation

Some of these tests were conducted at component levels before the motor final assembly.

In order to characterize the thermal performance of the rotor cryostat, two pairs of cryogenic temperature sensors are mounted at strategic locations as shown in Fig. 5.

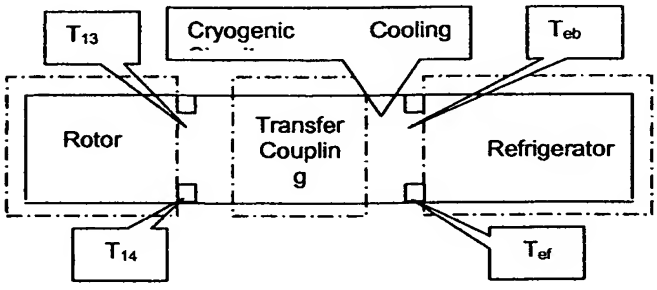

Figure 5. Location of cryogenic temperature sensors.

Losses at cryogenic temperature, or as they are commonly referred to as heat leak, are attributed to the refrigeration load. Heat leak calculations are based on temperature readings from the cryogenic temperature sensors and mass flow rate of cold helium gas circulating through the cooling circuit. Thermodynamic properties of helium gas used for heat leak calculation were generated from a database at measured temperatures. Temperature sensors T_{13} and T_{14} are mounted at the inlet and outlet of the cooling circuit to the rotor cryostat, respectively. Readings from this pair of temperature sensors are logged automatically by the DAQ system. These readings are used to generate enthalpy values for helium gas at the sensor locations, which are then used for calculating heat leak into the rotor cryostat using the following equation,

$$\dot{Q}_{rotor} = \dot{m}(h_{14} - h_{13}) \quad (1)$$

Similarly, the total heat leak into the system, including the transfer coupling and vacuum jacketed transfer lines, is calculated using enthalpy values corresponding to readings from temperature sensors T_{eb} and T_{ef} mounted at the inlet and outlet of the refrigerator. The overall heat leak into the system is therefore calculated as

$$\dot{Q}_{total} = \dot{m}(h_{ef} - h_{eb}) \quad (2)$$

VII. DATA ANALYSIS AND PERFORMANCE EVALUATION

The no-load test was conducted by running excitation current through the field winding while line to line voltage of the stator winding was measured. Line-to-line voltages, measured as function of excitation current, are presented in Table III.

TABLE III
VOLTAGE AS FUNCTION OF EXCITATION CURRENT

Excitation Current, A	A-B	B-C	C-A	Ave.
10	354.8	354.8	354.7	354.7
20	715.6	715.6	715.4	715.5
30	1077	1077	1077	1077
60	2164	2164	2163	2164
80	2885	2886	2885	2886
100	3606	3606	3605	3606
120	4328	4328	4327	4328

Corresponding to a rated stator voltage of 4,160 V, a no-load, rated field current can be interpolated as

$$I_o = 115.34\,A \quad (3)$$

The average values of the measurement deviate from theoretical prediction by no more than 3.5%, presumably due to construction variation in end regions. Experimental data from the short-circuit test are tabulated in Table IV.

TABLE IV
STATOR CURRENT AS FUNCTION OF EXCITATION CURRENT

Excitation Current, A	A	B	C	Ave.
10	54.8	54.5	54.4	54.57
15	82.3	81.8	81.6	81.9
20	109.4	108.8	108.6	108.9
25	137.0	136.4	136.2	136.6
30	164.6	163.8	163.6	164.0

Based on a 97.38% efficiency, the input power to the motor is valued at 766 kW with a stator phase current of 106.3 A from a 4160 V power source. The motor was actually tested at 4270 V, which rendered a stator phase current of 103.5 A. The excitation current corresponding to this stator phase current can be interpolated from the average measured values as

$$I_k = 19.01\,A \quad (4)$$

The synchronous reactance, defined as

$$X_d = \frac{I_k}{I_o} \quad (5)$$

can then be calculated with a value of *0.165 Ω*.

Short-circuit losses were evaluated based on measured active stator winding resistance *Ra* at *348 K*, using the following equation

$$P_{sc} = 3I^2 R_a \quad (6)$$

For a stator current of 103.5 A and a measured value of Ra = 0.225 Ω, the short-circuit losses takes a value of 7.3 kW, compared to a predicted value of 6.9 kW. The deviation is attributed to additional length of stator winding in the end regions and variation in Litz wire cross section.

Motor losses are calculated based on averaged measurement of input and output of the motor (the number of measurements was significant enough to obtain correlative values), and motor efficiency is evaluated at the nominal rating of 1,000 hp.

TABLE V
PERFORMANCE OF HTS MOTOR

Input Power kW	Output Power kW	Losses kW	Efficiency %
787.0	766.4	20.6	97.38

Of the total losses, 4.7 kW was from the back iron, an additional loss of 8.2 kW took place in the end zone, losses due to friction and windage counted for 1.4 kW, and the rest was from the stator winding. The maximum output power achievable by this motor is limited by the allowable temperature in the stator winding. Motor efficiency as a function of output power is graphically presented in Fig. 6.

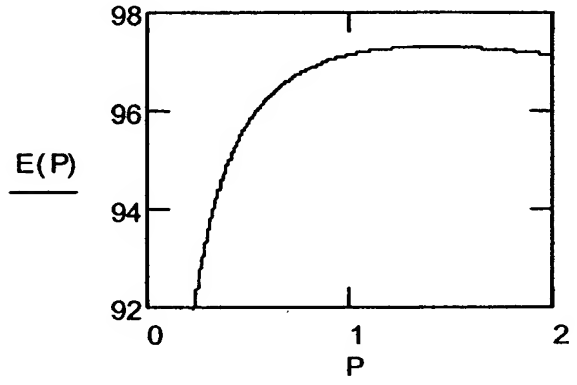

Figure 6. Efficiency of HTS motor as a function of output

This curve suggests that the motor would exhibit a higher efficiency in the overload regime (~1.5 times rated power), although direct measurement in this regime was not available.

The thermal performance of the rotor cryostat is summarized in Table VI.

TABLE VI
SUMMARY OF SYSTEM CRYOGENIC LOADS

Load Category	Cryogenic Load (W)
Parasitic	50.5
DC	3.5
Rotation	9.0
AC	16.6

Parasitic load comprises load due to heat transfer into the rotor cryostat via conduction and radiation through torque tubes, current leads, and vacuum space. DC load is the resistive term I^2R associated with the HTS field winding and current leads when they are energized. Load due to rotation is dissipative and mainly comes from the transfer coupling. AC load takes place in the field winding. Ideally, this term can be significantly reduced with a cold flux shield designed for a higher screening factor to prevent any AC element from reaching the field winding.

VIII. CONCLUSIONS

A *1,000-hp* HTS synchronous motor has been designed , built, and demonstrated which utilizes HTS field winding coils made of multifilament tape conductor. Cryogenic transfer couplings and helium cryocoolers have been developed in parallel efforts to support the HTS motor system testing. Valuable information has been gathered through the design and construction of this motor and will be applied to development of future large-scale HTS motor systems. Based on current HTS conductor technology, the performance of this motor reaches a break-even point where its efficiency becomes comparable with conventional motors taking into account the input power requirement of its cryogenic refrigeration system. Other significant conclusions from this effort are:

- The HTS motor delivered power at the designed level and was demonstrated at an overload of *60%.*
- The motor was demonstrated while operating from an adjustable speed drive (ASD). Results of these tests provided significant information for future HTS motor and drive system designs.
- The motor demonstration provided an operational verification of new novel system technologies and configurations, and opportunities for decreasing cryogenic loads and stray loss loads which will ultimately improve the system efficiency.
- The system remained in a cryogenic state nearly continuously for approximately one and a half years without any active pumping of the vacuum system.

Overall, this project has already either met or exceeded the program goals, and completion of this development will mark an important milestone in HTS motor technology. Significant efficiency improvement and volume reduction will be realized in the next *5,000-hp* HTS motor demonstration, where the goal is to have approximately half of the losses with half of the volume of the conventional motors.

REFERENCES

[1] Jordan, H., Feasibility Study of Electric Motors Constructed with High Temperature Superconducting Materials, *Electric Machines and Power Systems,* 16:15-23 (1989).

[2] Schiferl, R., et al., High Temperature Superconducting Synchronous Motor Design and Test, *Proc. of the American Power Conference,* Chicago, IL (1996).

[3] Zhang, B., et. al., Cryocooler Integration with High-Temperature Superconducting Motors, *proceedings of the 9th International Cryocooler Conference,* Plenum Press, New York, NY (1996).

[4] Shoykhet, B., Design of Composite Torque Tubes for High Temperature Superconducting Motors, *3rd U.S. Navy Symposium on Electrical Machines,* Philadelphia, 2000.